The College of Engineering
University of Wisconsin-Madison

Wisconsin Electric Machines and Power Electronics Consortium

RESEARCH REPORT
93-26

Influence of Current Waveshape on Motoring Performance of the Slotless Permanent-Magnet Machine Torus

Z. Dostal and B.J. Chalmers
UMIST, UK

T.A. Lipo
Dept. of Electrical and Computer Engineering
University of Wisconsin-Madison
1415 Johnson Drive
Madison, WI 53706

WEMPEC

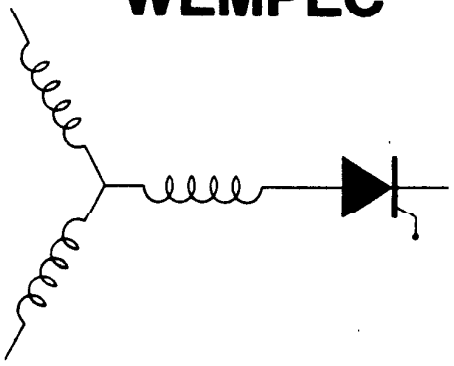

Department of Electrical and Computer Engineering
1415 Johnson Drive
Madison, Wisconsin 53706

IEE International Conference on Electrical Machines and Drives, Oxford, 1993.

INFLUENCE OF CURRENT WAVESHAPE ON MOTORING PERFORMANCE OF THE SLOTLESS PERMANENT-MAGNET MACHINE TORUS

Z. Dostal T.A. Lipo B.J. Chalmers

UMIST, UK University of Wisconsin, USA UMIST, UK

INTRODUCTION

The Torus machine is a double-sided, axial-flux, disc-type, permanent-magnet, brushless machine which may be operated as either a generator or a motor. Its particularly short axial length and good power-to-weight ratio is being exploited in a number of generator applications and there is now fairly widespread activity in the study of this machine topology both as generator (1-6) and as a motor (7-10). Early studies at UMIST and the University of Wisconsin specifically considered the operation of this type of machine as a brushless d.c. motor. Operation from a voltage source inverter with both six step square waveform (7) and pulse-width-modulation (8) were examined. As the Torus machine is equipped with single or double layer, full pitch uniformly distributed windings its open circuit emfs are far from sinusoidal. During these studies it was recognised that torque per ampere could be increased by matching the current waveshape to that of the trapezoidal emf, adopting the principle of instantaneous current regulation which has been successfully exploited in field-oriented control of induction machines. An investigation of improved methods of current regulation is reported in this paper based upon a 2.5kW, 24V, 9-phase machine previously developed as a generator.

SIMULATION STUDY

In order to evaluate the practicality of controlling a non-sinusoidal motor current, a complete digital computer simulation of the system was undertaken using the ACSL programming language. The approach to simulation was completely general in that all of the motor inductances and resistances were calculated directly in the simulation program from basic dimensions such as core cross section, gap distance, toroid inner and outer radius, wire diameter, etc. and also from design specifics such as winding turns and detailed winding placement in the air gap, magnet geometry, etc. Whereas conventional simulations neglect the higher spatial air gap MMF harmonics present in an ac machine, these higher harmonics have been retained in this study so as to correctly model the non-sinusoidal emf induced in the armature windings by the magnet. Figure 1 shows a simulated and measured waveform of the motor emf and indicates good correlation. The slight differences in the waveforms, in particular the slight slope on the top of the measured trapezoid, can be attributed to imperfections in the magnets. Slight differences in the positive and negative halves of the measured emf waveform can also be attributed to slight variations in the magnetization of the magnets. Figure 2(a) shows a typical steady-state current waveform as computed by ACSL. Comparison with Fig. 2(b) again indicates good agreement with tested results.

In general, it is desirable for the stator current waveform to match the emf as closely as possible so as to extract the best possible torque per rms ampere. Since the emf normally contains some triplen harmonics, it would be useful to employ a four-wire arrangement in order to supply the third harmonic current necessary to have the armature current precisely match the emf waveform. Unfortunately, normal switching of the inverter in such a case results in instances of time where all three of the phase legs of the motor are connected either to the positive or negative bus while the neutral is connected to the mid-point of the dc bus. In this case, the inductance seen by the inverter can be shown to be essentially 2/9 of the nominal value encountered by the inverter during normal three-wire switching, as suggested by Fig. 3. Hence, when compared to the three-wire case, a harmonic ripple current would flow of more than twice the three-wire nominal value when operating at the same basic PWM switching frequency.

Figure 4 shows computer simulation traces of a four-wire system which can be compared with Fig. 2. As suggested by the digital computer simulation study, control difficulties are introduced with a four-wire system since the current is not under active current regulation during an entire cycle. It was determined that very little additional torque is available from a four-wire system by utilizing the third harmonic component present in the emf waveform, at least for the machine under study. Hence, this configuration was rejected in favour of the three-wire system even though precise matching of emf and armature current waveform will not be possible in this case.

As for all machines with slotless windings, Torus has a very small stator leakage inductance. In addition, because of the large air gap, the magnetizing inductance is also relatively small. It was therefore also determined from simulation that current regulation using a hard-switched voltage-source inverter with a fixed dc link would require a very high switching frequency.

With switching at a more acceptable lower frequency (e.g. 12.5 kHz) the amplitude of current ripple was found to be excessive. One possible solution to this problem is to introduce a chopper in the dc link as shown in Fig. 5. By careful control of the chopper output voltage, the inverter dc input voltage can be controlled in such a manner that it differs from the internal emf of the motor by only a few volts, reducing greatly the slope of the instantaneous current during each switching instant and thereby influencing indirectly the modulation frequency of the current regulator loop. In the absence of a suitable voltage and current regulator, the objective of current waveshape control was achieved in this experimental study by simply inserting 10 mH inductance in series with each motor phase winding and these were incorporated into the simulation model which produced Figs. 2 and 4.

EXPERIMENTAL SYSTEM

The motoring studies of this paper have been conducted with appropriate sets of stator windings reconnected in series to form a 3-phase winding with increased voltage and reduced current ratings. The test rig arrangement used for this study is shown in Fig. 6. Hysteresis band control of the inverter output current was implemented to control its waveshape to match a demand waveshape. The current angle (MMF angle) was held constant at the optimum value of 90° for maximum torque, the Torus machine having no saliency. Three current waveshapes with the same peak amplitude of 9A were studied viz. (1) sinusoidal, (2) 60° flat top trapezoid, and (3) best fit to the measured open-circuit emf waveshape.

Figures 2(b), 7 and 8 show the demanded and measured current waveshapes for the cases where the current demand is sinusoidal, 60° flat top trapezoid and "best fit" to emf waveshape. Note that while very good correlation is obtained between the demanded and measured currents in Figs. 2(a) and 7, less accurate results are indicated in Fig. 8 owing to the fact that the current regulator is unable to completely zero the error since the demanded current contains a certain amount of third harmonic component in this case. It is important to note that whereas triplen harmonics produce purely leakage flux components in the case of a 3-wire, 3-phase machine they do contribute, however slightly, to torque production in a 4-wire, 3-phase machine having triplen space harmonics. Upon detailed examination, the errors resulting from inability to match the triplen harmonics were not deemed to be of importance since the resulting measured torque values were found to be essentially in accordance with predictions based on the product of current and emf waveshapes.

Figure 9 shows the products of the emf and current waveforms when the current is controlled to be one of the three waveshapes of Figs. 2(a), 7 and 8. Since the product of emf and current is equal to air gap power, the area under the curves of Fig. 9 is proportional to the average output torque times speed. Table 1 shows a comparison of the predicted and measured values of average torque. It can be noted that the predicted and measured values, relative to the sinusoidal-current case, correlate very well for the 60° trapezoid case. The measured value of torque produced by matching the armature current and emf waveforms is about 1.5% less than the ideal value; this may be attributed to the fact that triplen harmonic currents were not allowed to flow owing to the three-wire connection.

Table 1 Predicted and Measured Torques

Current Waveshape	Predictions area	relative (area/speed)	Measured Nm	relative
Sinusoidal	10915	1.000	1.89	1.00
Trapezoidal	11454	1.056	1.99	1.05
Same as emf	12471	1.127	2.10	1.11

CONCLUSION

This paper has demonstrated that additional torque can be extracted from an ac machine which is constructed so as to produce a non-sinusoidal emf. It has been shown that the characteristic full pitch, 60° phase spread winding of the Torus machine results in an additional 12.7% ideal, 11% actual improvement in torque-producing capability by matching the armature current to the induced emf when compared with the same machine fed with sinusoidal currents. Since the peak instantaneous current and voltage effectively determine the device rating of a power converter, it is apparent that operation in such a mode results in a 11% increase in the converter power rating without affecting the voltage or current rating of the converter switches. While this principle has been demonstrated for the Torus machine it is clear that it can be readily extended to other permanent-magnet or synchronous-reluctance motor configurations.

ACKNOWLEDGMENT

The work was conducted with support from SERC in the form of a Visiting Fellowship for Prof. Lipo.

REFERENCES

1. Rash N.M., Howe D., Spooner E.; 1985, Proc. IEE Int. Conf. 'Electrical Machines - Design and Applications', . 270-274.

2. Spooner E., Chalmers B.J.; 1988, Proc. Int. Conf. Electrical Machines, Pisa, 81-86.
3. Spooner E., Chalmers B.J.; 1990, Proc. Int. Conf. Electrical Machines, Cambridge, USA, 1054-1058.
4. Spooner E., Chalmers B.J.; 1992, IEE Proc. B, 139, 497-506.
5. Di Napoli A., Caricchi F., Crescimbini F., Noia G.; 1991, Proc. SM'100, Int. Conf. on the Evolution and Modern Aspects of Synchronous Machines, 1119-1123a.
6. Caricchi F., Crescimbini F., Honorati O., Santini E.; 1992, Proc. Int. Conf. on Elect. Machines, Manchester, 761-765.
7. Spooner E., Chalmers B.J., El-Missiry M.M., Wu Wei and Renfrew A.C; 1991, Proc. IEE Conf. Electrical Machines and Drives' 36-40.
8. Jensen C.C., Profumo F, Lipo T.A.' 1992, IEEE Trans. Ind. Applic., 28, 646-651.
9. Caricchi F., Crescimbini F., Di Napoli A., Honorati O., Lipo T.A., Noia G., Santini E.; 1991, Proc. IV European Conference on Power Electronics and Applications, 3, 482-487.
10. Caricchi F., Crescimbini F., Di Napoli A., Santini E.; 1992, Proc. Int. Conf. on Elect. Machines, Manchester, 637-641.

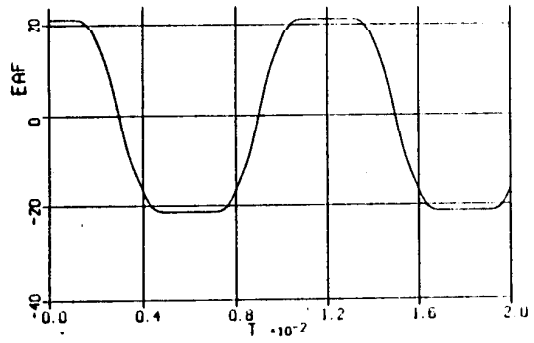

(a)

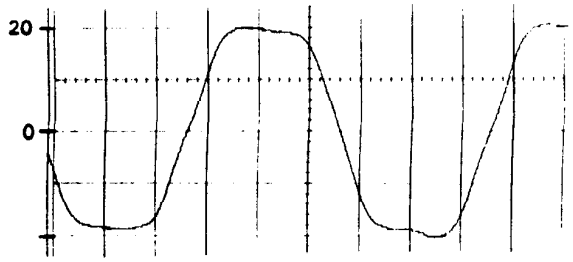

(b)

Fig. 1 (a) Simulated and (b) measured waveforms of motor emf at 1250 rpm.

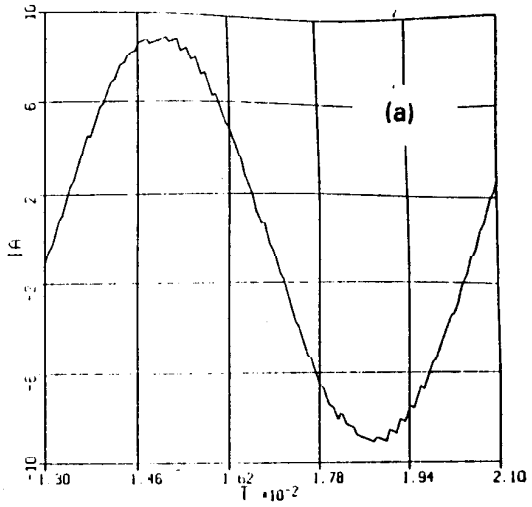

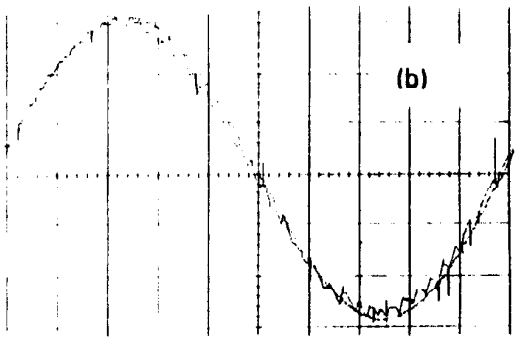

Fig. 2 Current waveforms for sinusoidal excitation.
(a) simulation, (b) test demand and measured. Maximum current demand I_m = 9.0A, dc link voltage V_{dc} = 150 V, electromagnetic torque T_e(ave) = 1.89 Nm, speed = 1996 rpm.

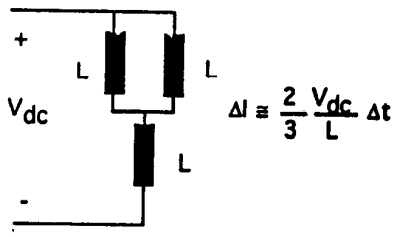

(a)

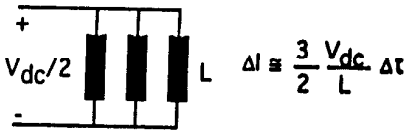

(b)

Fig. 3 Typical circuit connections for (a) three- and four-wire connection and (b) four-wire connection only.

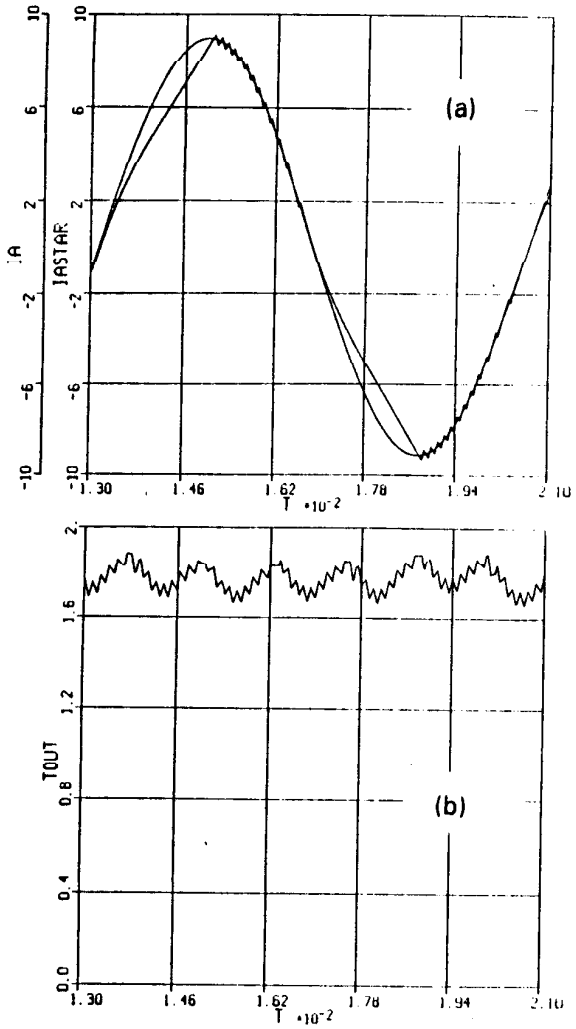

Fig. 4 Simulation results for four-wire connected machine. (a) phase current demand and resultant current, (b) electromagnetic torque.

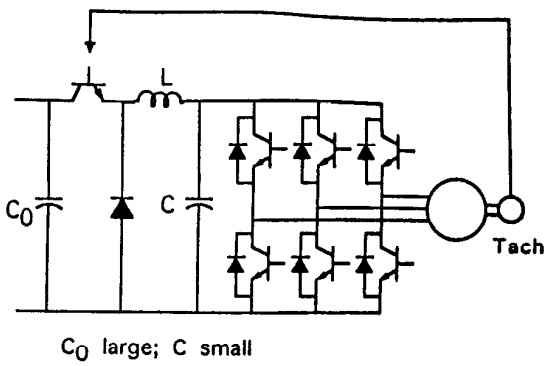

Fig. 5 Chopper circuit for controlling inverter dc link voltage as a function of speed.

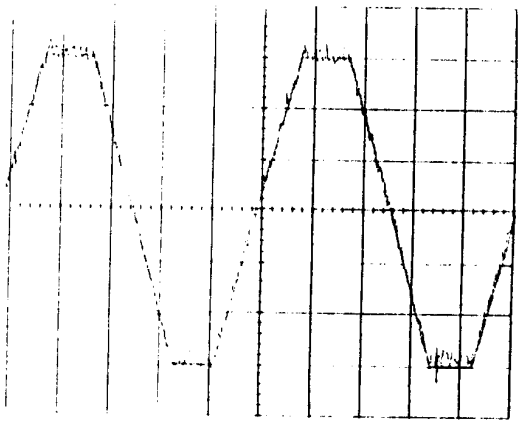

Fig. 7 Demand and measured current waveshapes for case of trapezoidal excitation.
Maximum current demand I_m = 9.0A, dc link voltage V_{dc} = 150 V, electromagnetic torque T_e(ave) = 1.99 Nm, speed = 1984 rpm.

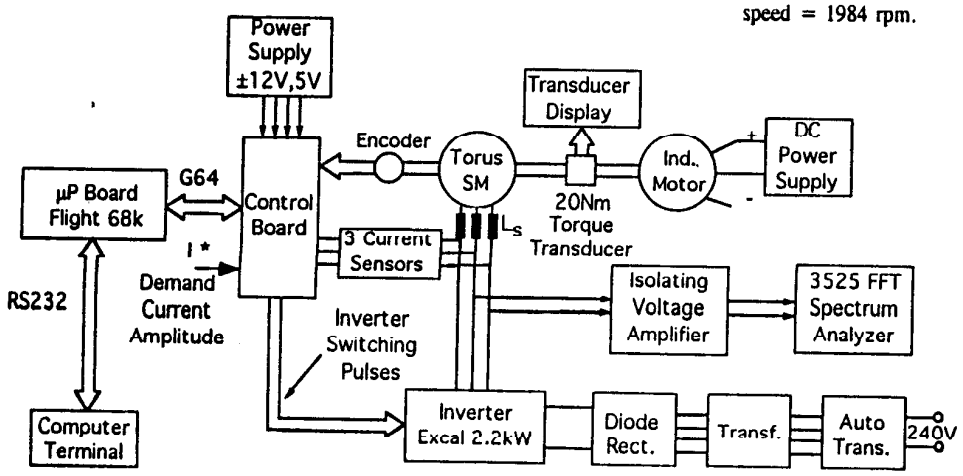

Fig. 6 Test rig arrangement

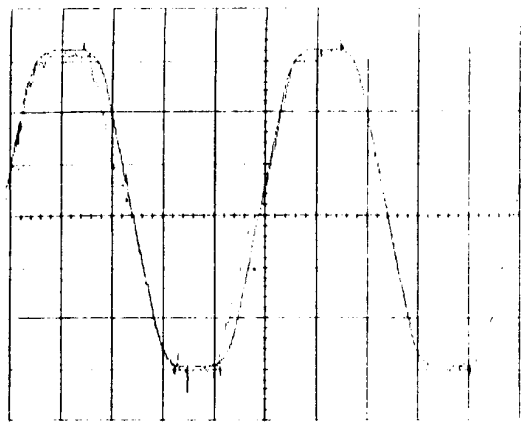

Fig. 8 Demand and measured current waveshapes when demand stator current has the same form as the emf.
Maximum current demand I_m = 9.0A, dc link voltage V_{dc} = 150 V, electromagnetic torque T_e(ave) = 2.1 Nm, speed = 2023 rpm.

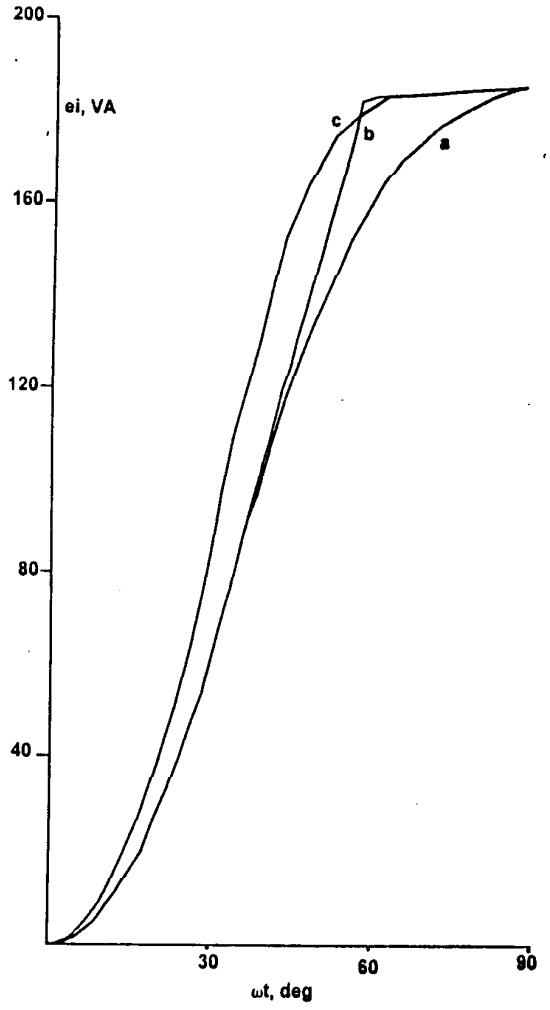

Fig. 9 Products of emf and phase current waveforms.
a - emf x sinusoid
b - emf x trapezoid
c - emf x emf